Fast removal of ammonium nitrogen from aqueous solution using chitosan-*g*-poly(acrylic acid)/attapulgite composite

Yian Zheng, Junping Zhang, Aiqin Wang*

Center of Eco-materials and Green Chemistry, Lanzhou Institute of Chemical Physics, Chinese Academy of Sciences, Tianshui Middle Road, No. 18, Lanzhou 730000, PR China

ARTICLE INFO

ABSTRACT

In this work, a novel composite adsorbent with three-dimensional cross-linked polymeric networks based on chitosan (CTS) and attapulgite (APT) was prepared via *in situ* copolymerization in aqueous solution, and its efficacy for removing ammonium nitrogen (NH_4^+-N) from synthetic wastewater was investigated using batch adsorption experiments. In the adsorption test, the pH effect, adsorption kinetics, isotherms, and desorbability were examined. A comparison between as-prepared adsorbent and clay, powdered activated carbon (PAC), and other reported adsorbents was also carried out. The results indicate that as-prepared composite adsorbent is pH-dependent and has faster adsorption kinetics and higher adsorption capacity. At natural pH, the composite adsorbent with 20 wt.% APT can adsorb 21.0 mg NH_4^+-N per gram, far higher than the other adsorbents involved. The adsorbed NH_4^+-N can be completely desorbed by 0.1 mol/L NaOH within 10 min. All information obtained give an indication that the composite can be used as a novel type, fast-responsive and high-capacity sorbent material for NH_4^+-N removal.

© 2009 Elsevier B.V. All rights reserved.

1. Introduction

Eutrophication of water bodies is a major, global environmental problem. Its main cause is disposal of nutrients (N and P) directly from water plants or indirectly from agriculture and leaching from sludge deposited in landfill and fields. Ammonium nitrogen (NH_4^+-N) is a very common chemical form in aquatic ecosystems and its toxic effect on life has been widely reported [1–5]. Higher ammonium levels found in natural waters are indicative of deteriorated water quality, especially due to accelerated anthropogenic activity. Total removal or at least a significant reduction of NH_4^+-N is thus obligatory prior to disposal into streams, lakes, seas and land surface. Up to now, the main NH_4^+-N removal processes involve biological nitrification, denitrification, air stripping, chemical treatment and selective ion exchange [6–9].

Adsorption, as one of the most economical promising techniques, has been used extensively in removing some toxic waste present in water [10,11]. Adsorbent materials, as the key factor in adsorption technology, should be attracted much attention. Activated carbon undoubtedly is known and regarded as the most popular adsorbent and has been widely used in wastewater treatment [12]. But, its higher cost of manufacturing and regeneration limit its large-scale application. As a consequence, numerous low-cost natural or modified clays have been focused as promising alternatives, however, their adsorption capacities are too low to satisfy the effective demand [13].

In recent years, polysaccharide-based adsorbents have been gaining acceptance [14], and hydrogels derived from polysaccharides have been used as alternative adsorbents for dyes removal from aqueous solution [15]. Hydrogels are slightly cross-linked hydrophilic polymers with excellent three-dimensional structured polymeric networks consisting of flexible chains. Multifunctional ionic groups within the hydrogels afford them surprising affinity to some metal ions or ionic dyes [16]. However, to the best of our knowledge, there is little literature focusing on the adsorption of NH_4^+-N onto hydrogels based on polysaccharides and clays. Chitosan-*g*-poly(acrylic acid)/attapulgite (CTS-*g*-PAA/APT) is an excellent composite adsorbent which can be easily prepared via *in situ* copolymerization in aqueous solution. Also, the resulting product is granular which is very different from common polymeric hydrogels with the formation of gel-form product requiring drying and crushing. This type of adsorbent has been prepared, optimized and well characterized in our previous study [17]. This work is a continuation of previous work and is mainly aimed at its application for NH_4^+-N removal from aqueous solution, which has not been well reported. The effects of various system parameters, such as pH values of initial NH_4^+-N solutions, contact time, NH_4^+-N concentration, and composition of adsorbent (i.e. APT content) were systematically investigated. The adsorption kinetics, isotherms and mechanism of NH_4^+-N onto CTS-*g*-PAA/APT were also proposed.

* Corresponding author. Tel.: +86 931 4968118; fax: +86 931 8277088.
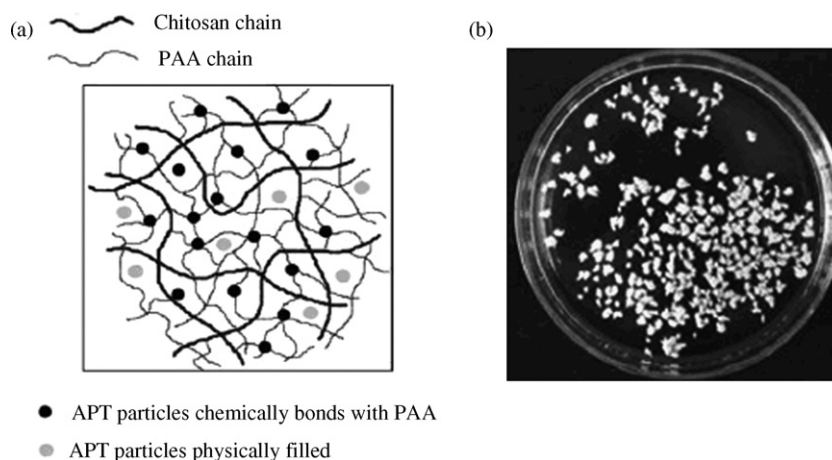*E-mail address:* aqwang@lzb.ac.cn (A. Wang).

Fig. 1. Schematic structure (a) and digital photo of CTS-g-PAA/APT composite (b).

2. Experimental

2.1. Materials

Acrylic acid (AA, chemically pure, Shanghai Shanpu Chemical Factory, Shanghai, China) was distilled under reduced pressure before use. Ammonium persulfate (APS, analytical grade, Xi'an Chemical Reagent Factory, Xi'an, China), N,N'-methylene-bisacrylamide (MBA, chemically pure, Shanghai Chemical Reagent Factory, Shanghai, China), chitosan (CTS, with an degree of deacetylation of 0.85 and average molecular weight of 3×10^5, Zhejiang Yuhuan Ocean Biology Co., Zhejiang, China), and powdered activated carbon (PAC) were used as received. Attapulgite (APT, Aotebang International Co., Jiangsu, China) and other clays, including montmorillonite (MMT, Longfeng Montmorillonite Co., Shandong, China), kaolin (Longyan Colloidal Co., Ltd., Fujian, China) and rectorite (Mingliu Rectorite Science and Technology Co., Ltd., Wuhan, China) were milled through a 200-mesh screen prior to use.

Nessler reagent. Dissolve 16 g of sodium hydroxide in 50 mL of water and then cool the solution to room temperature. Dissolve 10 g of red mercuric iodide and 7 g of potassium iodide in 40 mL of water, and then pour the iodide solution into the hydroxide solution under stirring, and dilute with water to 100 mL in a brown bottle. Allow to settle overnight, the clear supernatant liquid is used as the reagent.

2.2. Preparation and characterization of CTS-g-PAA/APT

An appropriate amount of CTS was dissolved in 1% (v/v) acetic acid in a 5 L double-layer glass reactor kettle equipped with a stirrer, a condenser, a thermometer and a nitrogen line. After removal of oxygen, the solution was heated to 60 °C gradually under nitrogen atmosphere while APS was added to initiate CTS to generate radicals. Then, the mixture consisting of AA, MBA and calculated amount of APT was put into the reaction kettle. The

solution was stirred at 70 °C for 3 h to complete the polymerization reaction. After that, the resulting granular product was neutralized with sodium hydroxide solution to pH 6–7, dehydrated with industrial alcohol and dried at 70 °C to a constant weight. The resulting adsorbent was milled through a 200-mesh screen prior to use. During the experiment, the weight ratio of MBA, APS and CTS in the feed was 3 wt.%, 2 wt.% and 10 wt.%, respectively. The preparation procedure of CTS-g-PAA was similar to that of the composite except without APT. The schematic structure and digital photo of CTS-g-PAA/APT composite were shown in Fig. 1.

FTIR spectra (Thermo Nicolet NEXUS™ spectrophotometer) showed that the graft reaction had taken place among CTS, AA and APT; morphological analysis (JSM-5600LV, JEOL, Ltd.) indicated that an appropriate addition of APT into the composite can form a relatively loose and fibrous surface [17]. However, excessive APT particles would act as the filler in the polymeric networks. The BET specific surface area and average pore size of the samples were measured using an Accelerated Surface Area and Porosimetry System (Micromeritics, ASAP 2020) by BET method at 76 K, and the results were shown in Table 1.

The point of zero charge (pH$_{PZC}$) of as-prepared adsorbent was determined by the solid addition method [18]. To a series of 100 mL conical flasks 45 mL of KNO$_3$ solution of known strength was transferred. The pH$_0$ values of the solution were roughly adjusted from 2 to 12 by adding either 0.1 mol/L HNO$_3$ or NaOH. The total volume of the solution in each flask was made exactly to 50 mL by adding the KNO$_3$ solution of the same strength. The pH$_0$ value of the solution was then accurately marked, and 0.1 g adsorbent was added, which was securely capped immediately. The suspensions were then manually shaken and allowed to equilibrate for 48 h with intermittent manual shaking. The pH values of the supernatant liquid were noted. The difference between the initial and final pH (pH$_f$) values (ΔpH = pH$_0$ − pH$_f$) was plotted against the pH$_0$. The point of intersection of the resulting curve at which ΔpH = 0 gave the pH$_{PZC}$, and the results were also shown in Table 1.

Table 1
Characteristics of as-synthesized adsorbent.

	Samples				
	CTS-g-PAA (0 wt.%)	CTS-g-PAA/APT (10 wt.%)	CTS-g-PAA/APT (20 wt.%)	CTS-g-PAA/APT (30 wt.%)	CTS-g-PAA/APT (50 wt.%)
Surface area (m²/g)	1.8277	8.3798	19.4058	24.6621	9.8539
Pore volume ($\times 10^2$ cm³/g)	0.4107	3.4261	7.3084	9.9477	2.8430
Pore size (nm)	8.9893	16.3542	15.0644	16.1344	11.5404
pH$_{PZC}$	5.07	5.09	5.13	5.09	5.07
Adsorption capacity (mg/g)	19.9	20.3	21.0	19.6	18.1

2.3. Adsorption experiment

A 1000 mg/L stock standard solution of NH_4^+-N was prepared by dissolving an appropriate amount of ammonium chloride (dried to constant mass at 100–105 °C) in 1000 mL of water. A series of working standard solutions were prepared by appropriate dilution of the stock solution. Other reagents used were all analytical grade and all solutions were prepared with distilled water.

Adsorption measurements were determined by batch experiment of 50 mg of the adsorbent with 25 mL of NH_4^+-N solutions. The mixtures were shaken in a thermostatic shaker (THZ-98A) at 30 °C/120 rpm for a given time, and then the suspensions were centrifuged at 4500 rpm for 10 min. The pH value was adjusted by adding 0.1 mol/L HCl or NaOH solution (Mettler Toledo 320 pH-meter). The experiments were carried out by varying pH of initial suspension (3.0–10.0), contact time (1–120 min), and initial NH_4^+-N concentration (25–1000 mg/L). The initial and final concentrations of NH_4^+-N in the solution were measured according to Nessler's reagent colorimetric method. The adsorption capacity for NH_4^+-N was calculated from the following equation:

$$q_e = \frac{(C_0 - C_e)V}{m} \tag{1}$$

where q_e is the adsorption capacity of NH_4^+-N onto adsorbent (mg/g), C_0 is the initial NH_4^+-N concentration (mg/L), C_e is the equilibrium NH_4^+-N concentration (mg/L), m is the mass of adsorbent used (mg), and V is the volume of NH_4^+-N solution used (mL).

During the competitive experiment, 50 mg hydrogel adsorbent was added into the mixing solution containing NH_4-N with the concentration of 100 mg/L and phosphate (PO_4-P) with the concentration of 100 mg/L. PO_4-P present in the solution was analyzed by ammonium molybdate spectrophotometric method (GB 11893-89, in Chinese).

To avoid the mercury contamination, the mercury-containing wastewater is collected into a plastic barrel and aerated when 20 L of wastewater is colleted. After that time, 50 mL 400 g/L NaOH solution and 50 g $Na_2S \cdot 9H_2O$ are added. 10 min later, 200 mL of commercially available H_2O_2 is added slowly. The wastewater is allowed to settle for 24 h, and then the residues can be discarded.

2.4. Desorption experiment

For desorption study, the adsorbent adsorbed NH_4^+-N was separated from the NH_4^+-N solution and washed gently with distilled water for several times. Then, NH_4^+-N-loaded adsorbent (50 mg) was agitated in a series of 50 mL conical flasks containing 25 mL of aqueous solution of HCl, NaOH and NaCl with known concentration of 0.1 mol/L or distilled water at room temperature for 2 h. Thereafter, the supernatant was analyzed for NH_4^+-N released into the eluent and an appropriate eluent was then selected.

Once an eluent was chosen, it is important to evaluate the desorption kinetics. In a series of NH_4^+-N-loaded adsorbents, 25 mL of chosen eluent was added. At set interval, the corresponding supernatant was analyzed for NH_4^+-N released into the eluent. The desorbed amount of NH_4^+-N was then obtained and the optimum desorption time was determined.

3. Results and discussion

3.1. Effect of pH on adsorption capacity

The amount of NH_4^+-N removed by CTS-*g*-PAA/APT and equilibrium pH values as a function of original pH were shown in Fig. 2. It can be seen from Fig. 2 that the equilibrium pH values are different from those original pH values after the adsorption. With increasing pH of the initial NH_4^+-N solution, the amount adsorbed for NH_4^+-
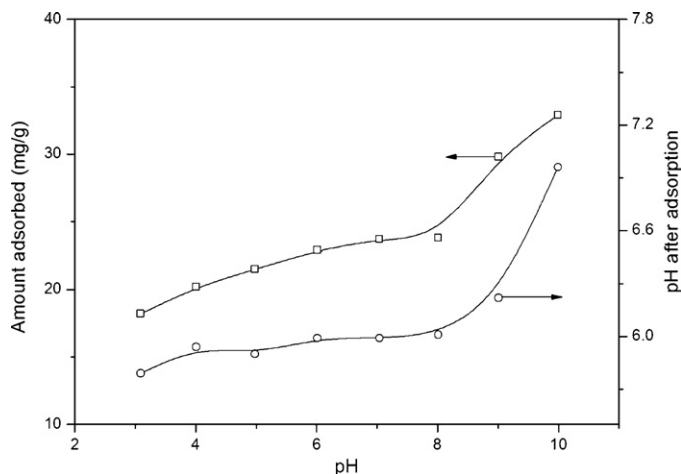

Fig. 2. Effect of pH on the adsorption capacity of NH_4^+-N onto CTS-*g*-PAA/APT (10 wt.%) ($T = 30$ °C, $t = 4$ h, $C_0 = 100$ mg/L, adsorbent dose = 50 mg/25 mL, 120 rpm).

N increases, especially when pH > 8.0. So, the pH values after the adsorption are considered to be the governing factor influencing the ionization degree of –COOH groups and then affect the amount adsorbed of CTS-*g*-PAA/APT for NH_4^+-N.

CTS is a weak base with an intrinsic pK_a of 6.5 and PAA contains carboxylic groups that become ionized at pH values above its pK_a of 4.7 [19]. In this work, most of the active amino groups of CTS have participated in the copolymerization [17]. Due to the low pK_a of PAA, –COOH groups can be easily ionized and the ionization degree increased with increasing external pH values. As illustrated in Fig. 2, with increasing the external pH values from 3.0 to 8.0, the equilibrium pH value increases gradually from 5.8 to 6.0, and further increase in external pH values can give final pH values of 6.2 and 7.0 when external pH value is 9.0 and 10.0, respectively. The changes in pH value before and after the adsorption may be arisen from the buffer action of –COOH and –COO$^-$ on the polymer chains of adsorbent [20]. So, it can be concluded that with increasing pH values of original NH_4^+-N solution from 3.0 to 8.0, the equilibrium pH values change slightly and beyond pH = 8.0, an obvious increase in equilibrium pH value is observed.

It is also observed from Fig. 2 that when pH value of original NH_4^+-N solution lies between 6.0 and 8.0, the adsorption capacity of as-prepared adsorbent for NH_4^+-N is almost the same, and furthermore, the original working standard NH_4^+-N solution in this study has a pH value of 6–7. Therefore, the pH value of working NH_4^+-N solution is not necessary to be adjusted, that is, the adsorption experiment can be carried out at "natural pH".

3.2. Effect of contact time on adsorption capacity

Contact time is an important parameter because this factor can reflect the adsorption kinetics of an adsorbent for a given initial adsorbate concentration. At natural pH, the effect of contact time on adsorption capacity was investigated, as shown in Fig. 3. The adsorption of NH_4^+-N onto CTS-*g*-PAA/APT as a function of contact time showed that the adsorption was very rapid and >90% could be achieved within 5 min. This fast kinetics between adsorbent and NH_4^+-N was attributed to the well-formed three-dimensional polymeric networks. As-prepared adsorbent belongs to hydrogels whose main feature is the ability to absorb water quickly due to the hydrophilic networks. After the initial faster hydration of the polymer network, concentration gradient of NH_4^+-N is formed at gel–water interface, thereby the diffusion of NH_4^+-N from the aqueous solution into the gel is started and bound immediately to the swollen polymeric networks as a result of electrostatic attrac-

Table 2
Estimated kinetic model parameters for NH_4^+-N adsorption.

First-order equation			Second-order equation			Power function equation			Elovich equation		
a	b	R^2	a	b	R^2	a	b	R^2	a	b	R^2
19.81	8.706E−1	0.9898	20.46	1.575	0.9729	15.13	6.854E−2	0.9027	14.74	1.325	0.9100

tion. Then, the adsorbate NH_4^+-N outward is moved at once into the swollen polymeric networks, leading the adsorption system to reach equilibrium within a few minutes.

Four typical kinetic equations were commonly used to fit the experimental data, as shown below [21]:

$$\text{First-order equation}: \quad q = a(1 - e^{-bt}) \tag{2}$$

$$\text{Second-order equation}: \quad q = \frac{abt}{1+bt} \tag{3}$$

$$\text{Power function equation}: \quad q = at^b \tag{4}$$

$$\text{Elovich equation}: \quad q = a + b\ln t \tag{5}$$

where q is the amount adsorbed (mg/g) and t is the adsorption time (min). The other parameters are different kinetics constants, which can be determined by regression of the experimental data. By non-linear regression, the corresponding kinetic parameters were summarized in Table 2. The parabolic diffusion equation and simple Elovich equation were ruled out because their correlation coefficients (R^2) for the present experimental data were poor. Based on the difference between the amount adsorbed at equilibrium and calculated, as well as correlation coefficient R^2, it is clearly observed that NH_4^+-N adsorption on the adsorbent can be satisfactorily described by first- and second-order equations. As mentioned earlier, the adsorption process was mainly controlled by the electrostatic attraction between NH_4^+-N and –COO$^-$ within the composite adsorbent. Therefore, the number of ionized groups was considered the major active adsorption sites for NH_4^+-N. This is consistent with the assumption proposed by first- and second-order equations. Based on these discussions, it can be concluded that the adsorption process of NH_4^+-N onto CTS-g-PAA/APT is greatly influenced by the amount of adsorbate on the surface of the adsorbent and the amount of adsorbate adsorbed at equilibrium, and the adsorption rate is directly proportional to the number of active adsorption sites on the surface of the adsorbent.
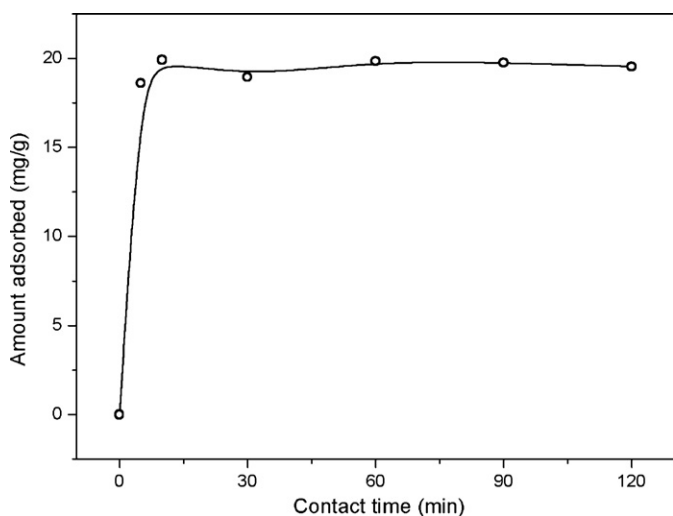

Fig. 3. Effect of contact time on the adsorption capacity of NH_4^+-N onto CTS-g-PAA/APT (10 wt.%) (T = 30 °C, C_0 = 100 mg/L, adsorbent dose = 50 mg/25 mL, natural pH, 120 rpm).

3.3. Effect of APT content on textural features and adsorption capacity

To understand the adsorption mechanism of NH_4^+-N onto this novel adsorbent, a series of adsorbent containing different APT content were prepared. It can be seen from Table 1 that compared with CTS-g-PAA, the surface area and pore volume of CTS-g-PAA/APT increased greatly up to respective maximum of 24.6621 m^2/g and 0.0995 cm^2/g, and then decreased sharply with further increase in APT content (50 wt.%). However, the adsorption average pore width showed different tendency, and the maximum pore size appeared to be 16.3542 nm when 10 wt.% APT was incorporated. This is due to that compared with CTS-g-PAA, an appropriate introduction of APT into the polymeric networks can form a relatively loose and fibrous surface, and also, a larger amount of micro-pores have been observed [17], making thus the product has a higher pore size. However, an excessive addition of APT would fill in the pore formed previously, i.e. excessive APT particles would act as the physical filler, and accordingly, the pore size would decrease. In this work, the pH_{PZC} value is assigned to CTS-g-PAA/APT with different APT content, and the determination value is located within 5.07–5.13, suggesting that the pH_{PZC} of this kind of adsorbent is independent on APT content, and the specific pH_{PZC} approximates 5.10. When the pH is lower than the pH_{PZC} value, the acidic water donates more protons than hydroxide groups, and so the adsorbent surface is positively charged (attracting anions). Conversely, above pH_{PZC} the surface of the composite adsorbent is negatively charged (attracting cations/repelling anions). The adsorption experiments in this work were performed at natural pH (6–7), and thus it is a favored process for the adsorption of NH_4^+-N onto CTS-g-PAA/APT.

The effects of APT content on NH_4^+-N removal were investigated. As summarized in Table 1, the amount adsorbed for NH_4^+-N increased with increasing APT content up to an optimum result of 20 wt.%, and then decreased with further increase in APT content. Thus, it can be deduced that the adsorption capacity is not in direct proportion to the surface area and porosity of the adsorbent. Although CTS-g-PAA/APT (30 wt.%) has the largest surface area and pore volume, it sorbs less NH_4^+-N than CTS-g-PAA/APT (20 wt.%), even less than that of CTS-g-PAA with smallest surface area and pore volume. As the hydrogels, as-prepared adsorbent possesses three-dimensional structural networks, which can contribute to final adsorption capacity, but not the governed factor. The sorption is credited to the presence of –COO$^-$ groups within the polymeric network. Sorption of NH_4^+-N onto this adsorbent is mainly controlled by the electrostatic attraction between the negative adsorption site of the adsorbent (–COO$^-$) and the positive charged NH_4^+-N. Owing to reactive –OH groups, an appropriate addition of APT would enlarge the surface area and porosity of the adsorbent and contribute to its better adsorption capacity. However, APT particles as the filler would produce significant negative effects on the adsorption capacity, i.e. the surface area and porosity of the adsorbent, especially the proportion of hydrophilic –COO$^-$ groups would decrease greatly, leading the final adsorption capacity to show a decreasing tendency. Nevertheless, incorporating 50 wt.% APT into the adsorbent, the adsorption capacity decreases only 2.9 mg/g than the maximum adsorption capacity of 21.0 mg/g (20 wt.% APT), however, the cost would reduce greatly.

In order to illustrate the potential of as-prepared composite adsorbent as an interesting adsorbent with higher adsorption

Table 3
The amount adsorbed for NH_4^+-N onto different adsorbents.

Adsorbents	Amount adsorbed	Reference
CTS-*g*-PAA/APT (20 wt.%)	21.0 mg/g	This study
Montmorillonite	7.8 mg/g	This study
Kaolin	5.5 mg/g	This study
Attapulgite	8.5 mg/g	This study
Rectorite	6.4 mg/g	This study
PAC	5.7 mg/g	This study
Natural zeolite	1.0–1.5 mg/g	[13]
Clinoptilolite	0.64 mequiv./g	[22][a]
Zeolite 13X	8.61 mg/g	[23][a]
Activated sludge	0.4–0.5 mg/g	[24][a]
NIPA	5.73 μmol/g	[25][b]
NIPA-CH	12.89 μmol/g	[25][b]

[a] Maximum sorption capacity.
[b] Low-concentration NH_4^+-N, NIPA and NIPA-CH represent poly(*N*-isopropylacrylamide) and poly(*N*-isopropylacrylamide-co-chlorophyllin), respectively.

capacity and faster adsorption kinetics, in the current work, the adsorption capacities of various clays and powdered activated carbon were also investigated under the same adsorptive conditions and compared with as-prepared composite adsorbent [22–25], as listed in Table 3. The adsorption capacity of as-prepared adsorbent was found to be 21.0 mg/g, 2–4 times higher than those clay adsorbents and PAC. In addition, the comparison between as-prepared adsorbent and other reported adsorbents was performed. It is clear that the adsorption capacity of developed adsorbent is much higher than those reported adsorbents for removing NH_4^+-N and is superior to Zeolite 13X. The higher adsorption capacity of as-prepared adsorbent is related closely to its composition and structure. The affinity of CTS-*g*-PAA/APT towards water is beneficial to its faster swelling properties and thus the concentration gradient of NH_4^+-N is formed at gel–water interface, which can promote to its faster adsorption kinetics for NH_4^+-N removal. The functional anionic groups (such as –COO$^-$ groups) is the reliable parameter for representing the adsorption capacity of as-prepared adsorbent for NH_4^+-N removal. All the information obtained suggests the effectiveness of developed CTS-*g*-PAA/APT superabsorbent as a potential adsorbent for NH_4^+-N removal in water.

3.4. Adsorption isotherms

The adsorption of NH_4^+-N onto CTS-*g*-PAA/APT determined as a function of equilibrium NH_4^+-N concentration is plotted in Fig. 4. It can be seen that the absolute amount of NH_4^+-N removed increased firstly with an increase in equilibrium NH_4^+-N concentration, thereafter, a little decrease was observed. This is due to that an increase in NH_4^+-N concentration accelerates the diffusion of NH_4^+-N molecules onto the adsorbent as a result of an increase in the driving force of concentration gradient. With the progress of adsorption, the availability of adsorption sites of the adsorbent gets diminished, leading thus the adsorption capacity to be constant. However, the weak binding between adsorbent and adsorbate makes the adsorption capacity show a little decrease. During the experiment, it has found that the initial pH value of NH_4^+-N solution decreases with increasing initial NH_4^+-N concentration, which may also be responsible for decreasing adsorption capacity when higher-concentration NH_4^+-N is employed.

The adsorption isotherms reveal the specific relation between the concentration of adsorbate and the adsorption capacity of an adsorbent at a constant temperature. In this study, three important isotherms are selected, that is, Langmuir, Freundlich and Dubinin–Radushkevich (D-R) models.

The Langmuir isotherm assumes that the adsorption occurs at specific homogeneous sites on the adsorbent and is the most commonly used model for monolayer adsorption process, as represented by the following equation [26]:

$$q_e = \frac{q_m b C_e}{1 + b C_e} \tag{6}$$

where q_e is the equilibrium adsorption capacity of NH_4^+-N on adsorbent (mg/g), C_e is the equilibrium NH_4^+-N concentration (mg/L), q_m is the monolayer adsorption capacity of the adsorbent (mg/g) and b is the Langmuir adsorption constant (L/mg). These parameters can be determined by non-linear regression of the experimental data.

The Freundlich isotherm equation, the most important multilayer adsorption isotherm for heterogeneous surfaces, is described by the following equation [27]:

$$q_e = K C_e^{1/n} \tag{7}$$

where q_e is the equilibrium adsorption capacity of NH_4^+-N on adsorbent (mg/g), C_e is the equilibrium NH_4^+-N concentration (mg/L), K is a constant related to the adsorption capacity and $1/n$ is an empirical parameter related to the adsorption intensity, which varies with the heterogeneity of the adsorption material.

The equilibrium was also applied to D-R model, which is more generally used to distinguish between physical and chemical adsorption, given by the following equation [28]:

$$\ln q_e = K\varepsilon^2 + \ln q_m \tag{8}$$

where q_e is the amount adsorbed for NH_4^+-N (mg/g), q_m is the maximum adsorption capacity of NH_4^+-N on the adsorbent (mg/g), K is the D-R constant (mol^2/J^2) and ε is the Polanyi potential and equals to $\varepsilon = RT\ln(1 + (1/C_e))$, where R (J/(mol K)) is the gas constant and T (K) is the absolute temperature. Thus the plot of $\ln q_e$ against ε^2 gives a straight line with a slope of K and an intercept of $\ln q_m$. The constant K can give valuable information regarding the mean free energy E (kJ/mol) of sorption per molecule of sorbate, and E can be obtained using the following relationship:

$$E = \frac{1}{\sqrt{-2K}} \tag{9}$$

In this study, the experimental data were fitted to the above three important isotherms by non-linear regression and the estimated model parameters with correlation coefficient (R^2) were
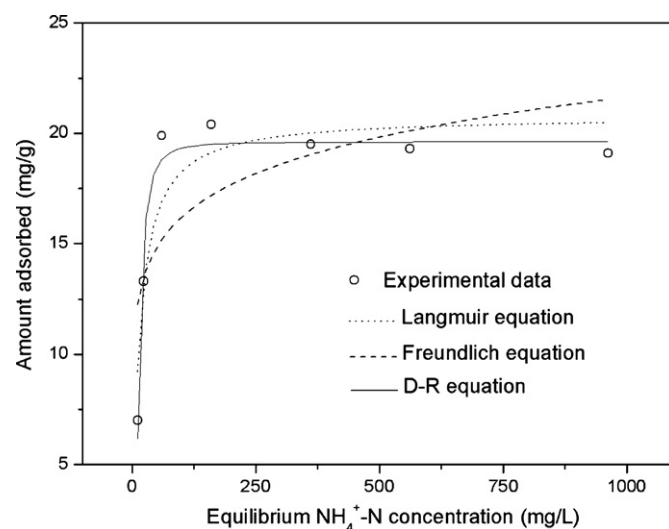

Fig. 4. The change of adsorption capacity as a function of equilibrium NH_4^+-N concentration ($T = 30$ °C, $t = 30$ min, adsorbent dose = 50 mg/25 mL, natural pH, 120 rpm, 10 wt.% APT).

Table 4
Parameters of Langmuir, Freundlich and D-R isotherms.

Langmuir equation			Freundlich equation			D-R equation		
q_m	b	R^2	K	n	R^2	q_m	K	R^2
20.76	7.31E−2	0.8755	9.080	7.96	0.5516	19.62	−2.00E−5	0.9610

summarized in Table 4. The fitting curves from the three isotherms were also illustrated in Fig. 4. The correlation coefficient for D-R model is the highest in comparison to values obtained from other isotherms and Freundlich model gives the poorest fit of experimental data. Therefore, D-R isotherm is the best-fit isotherm equation for the adsorption of NH_4^+-N onto CTS-*g*-PAA/APT composite adsorbent. Then *E* would be calculated from D-R isotherm and was used to estimate the adsorption mechanism. If the *E* value is between 8 kJ/mol and 16 kJ/mol, the adsorption process follows by chemical ion exchange, whereas if *E* lies between 1 kJ/mol and 8 kJ/mol, the adsorption is controlled by a physical adsorption [29]. The mean adsorption energy is calculated as 0.158 kJ/mol for the adsorption of NH_4^+-N onto CTS-*g*-PAA/APT, indicating that the adsorption process is not governed by the above proposed adsorption mechanism which is consistent with previous discussions, that is, the adsorption process is mainly controlled by the electrostatic attraction between negative adsorption site of the adsorbent ($-COO^-$) and the positive charged NH_4^+-N.

3.5. Desorption and regeneration

Desorption studies is helpful in elucidating the mechanism of an adsorption process. If NH_4^+-N adsorbed onto the adsorbent can be desorbed by water, it can be said that the attachment of NH_4^+-N onto the adsorbent is by weak bonds. If the strong acid or strong base, such as HCl or NaOH can desorb the NH_4^+-N, it can be said that the attachment of NH_4^+-N onto the adsorbent is by electrostatic attraction or ion exchange [18]. In this study, various eluents including distilled water, HCl, NaOH and NaCl were selected and the results suggested that, 16.1% of NH_4^+-N can be desorbed by water, 95.5% of NH_4^+-N can be desorbed by 0.1 mol/L NaCl, and the adsorbed NH_4^+-N can be completely desorbed by 0.1 mol/L HCl or NaOH. This information means that the attachment of NH_4^+-N onto CTS-*g*-PAA/APT is mainly by electrostatic attraction. Thereafter, 0.1 mol/L NaOH was selected as the eluent to investigate desorption kinetics (Fig. 5). Desorption time is an important condition for ensuring that NH_4^+-N can be completely desorbed

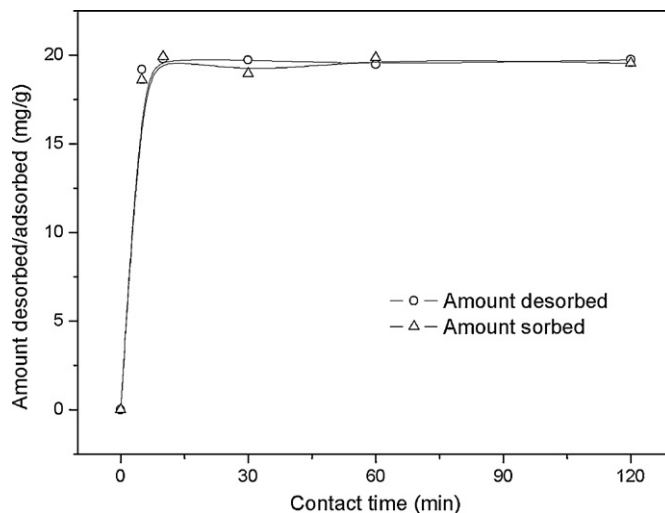**Fig. 5.** Variation of amount desorbed/adsorbed for NH_4^+-N as a function of contact time. Adsorption conditions: $T = 30$ °C, $C_0 = 100$ mg/L, adsorbent dose = 50 mg/25 mL, natural pH, 120 rpm; desorption conditions: 25 mL 0.1 mol/L NaOH, magnetic stirring.

from the surface of composite adsorbent, which can be determined from the measurement of desorption kinetics, amount desorbed against contact time. The results imply that desorption kinetics are found to show the same tendency with adsorption kinetics, and both kinetic curves are almost overlapped. The amount desorbed of NH_4^+-N from CTS-*g*-PAA/APT as a function of contact time show that desorption process was very rapid and >95% could be achieved within 5 min, suggesting that as-prepared adsorbent can be easily regenerated and then be used again. Based on the discussions above, it can be concluded that during the adsorption, two adsorption processes exist: pore-adsorption (small fraction) arose from three-dimensional structural networks of the adsorbent and electrostatic attraction (controlled larger fraction) between
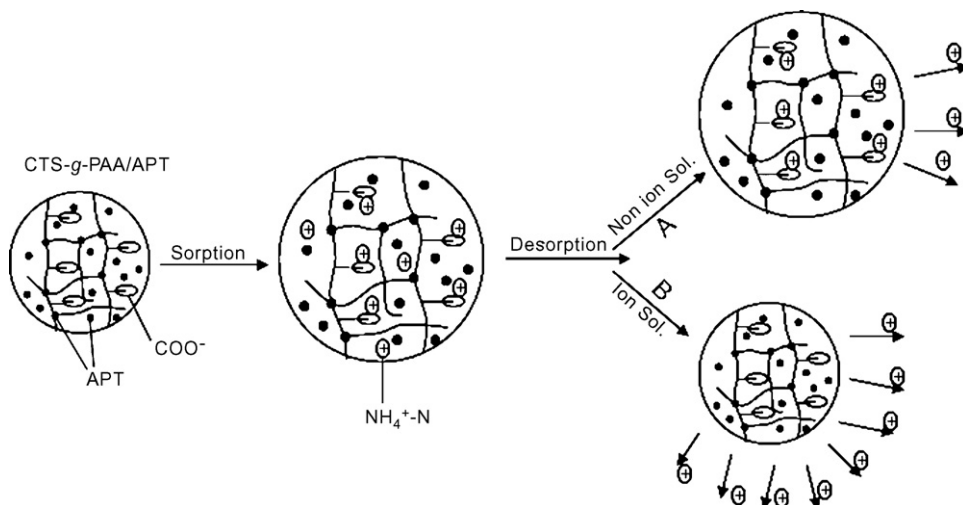

Fig. 6. Model scheme for the adsorption/desorption of NH_4^+-N onto/from CTS-*g*-PAA/APT polymeric networks. Non-ion sol., distilled water; Ion sol., 0.1 mol/L HCl (NaOH or NaCl); A, NH_4^+-N release of three-dimensional network adsorption; B, NH_4^+-N release of electrostatic adsorption.

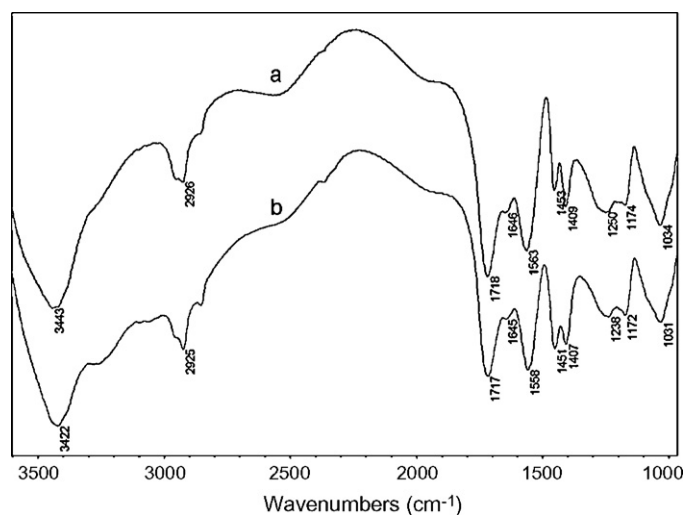**Fig. 7.** FTIR spectra of CTS-*g*-PAA/APT (10 wt.% APT) before (a) and after (b) adsorption for NH$_4^+$-N.

adsorbent and adsorbate. Corresponding model scheme for the adsorption/desorption of NH$_4^+$-N onto/from CTS-*g*-PAA/APT polymeric network can be observed in Fig. 6.

3.6. Adsorption mechanism

During the adsorption process, the electrostatic attraction can be testified by performing the adsorption experiment in a mixed solution containing positively charged NH$_4^+$-N and negatively charged PO$_4^{3-}$-P (orthophosphate). The results indicate that after the adsorption, the residual PO$_4^{3-}$-P concentration in the solution equals to the original PO$_4^{3-}$-P concentration, that is, in the mixed solution containing NH$_4^+$-N and PO$_4^{3-}$-P, CTS-*g*-PAA/APT can exclusively absorb NH$_4^+$-N while PO$_4^{3-}$-P is remained. This is the strong evidence that the electrostatic attraction is responsible for the adsorption of NH$_4^+$-N onto CTS-*g*-PAA/APT.

In order to further illustrate the adsorption mechanism of as-prepared composite adsorbent, in current work, Fig. 7 represents the FTIR spectra of CTS-*g*-PAA/APT (10 wt.% APT) before and after adsorption of NH$_4^+$-N. It can be seen that the main absorption peaks of CTS-*g*-PAA/APT can be observed on the spectrum after adsorption as compared to that of CTS-*g*-PAA/APT before adsorption, except a slight shift of asymmetric –COO$^-$ stretching from 1563 cm^{-1} to 1558 cm^{-1} and some changes in absorption band intensity of symmetric –COO$^-$ stretching at 1453 cm^{-1}. This information implies that after the adsorption, the surrounding environment of –COO$^-$ has changed, that is, the adsorption process between NH$_4^+$-N and CTS-*g*-PAA/APT is mainly controlled by the electrostatic attraction and may not involve a chemical interaction.

4. Conclusions

In this study, the potential of CTS-*g*-PAA/APT composite for NH$_4^+$-N removal from aqueous solution was evaluated. The hydrophilic anionic groups and three-dimensional structured polymeric networks are responsible for its higher adsorption capacity and faster adsorption kinetics for NH$_4^+$-N removal. First-order and second-order equations can well describe the adsorption kinetics, meaning that the adsorption rate is directly proportional to the number of active adsorption sites on the surface of the adsorbent. D-R isotherm is better to fit the experimental data compared with commonly used Langmuir and Freundlich models. Electrostatic attraction between the negative adsorption site of the adsorbent (–COO$^-$) and the positive charged adsorbate is the governing

mechanism for NH$_4^+$-N removal. Incorporating 50 wt.% APT into the adsorbent, the adsorption capacity decreases only 2.9 mg/g than the adsorbent with highest adsorption capacity (20 wt.% APT, 21.0 mg/g), however, the cost would reduce remarkably. This adsorbent can be easily regenerated, and resulting NH$_4^+$-N-loaded adsorbent can be considered as the fertilizer to be used in the field of agriculture owing to its unique water-retention characteristic and multi-functionality.

References

[1] L. Guo, Doing battle with the green monster of Taihu Lake, Science 317 (2007) 1166.
[2] G.T. Ankeley, M.K. Schubauer-Berigan, P.D. Monson, Influence of pH and hardness on toxicity of ammonia to the amphipod *Hyalella azteca*, Can. J. Fish. Aquat. Sci. 52 (1995) 2078–2083.
[3] D.P. Monda, D.L. Galat, S.E. Finger, Evaluating ammonia toxicity in sewage effluent to stream macroinvertebrates. I. A multi-level approach, Arch. Environ. Contam. Toxicol. 28 (1995) 378–384.
[4] J.R. Caicedo, N.P. Van Der Steen, O. Arce, H.J. Gijzen, Effect of total ammonia nitrogen concentration and pH on growth rates of duckweed (*Spirodela polyrrhiza*), Water Res. 34 (2000) 3829–3835.
[5] J. Puigagut, H. Salvadó, J. García, Short-term harmful effects of ammonia nitrogen on activated sludge microfauna, Water Res. 39 (2005) 4397–4404.
[6] R. Sedlack, Phosporous and Nitrogen Removal from Municipal Wastewater: Principles and Practice, second ed., Lewis Publisher, New York, 1991.
[7] W.P. Barber, D.C. Stuckey, Nitrogen removal in a modified anaerobic baffled reaction (ABR). 1. Denitrification, Water Res. 34 (2000) 2413–2422.
[8] S. Leaković, I. Mijatović, Š. Cerjan-Stefanović, E. Hodžić, Nitrogen removal from fertilizer wastewater by ion exchange, Water Res. 34 (2000) 185–190.
[9] X.Z. Li, Q.L. Zhao, Efficiency of biological treatment affected by high strength of ammonium-nitrogen in leachate and chemical precipitation of ammonium-nitrogen as pretreatment, Chemosphere 44 (2001) 37–43.
[10] L. Wang, A. Wang, Adsorption characteristics of Congo Red onto the chitosan/montmorillonite nanocomposite, J. Hazard. Mater. 147 (2007) 979–985.
[11] W. Wang, H. Chen, A. Wang, Adsorption characteristics of Cd(II) from aqueous solution onto activated palygorskite, Sep. Purif. Technol. 55 (2007) 157–164.
[12] E. Okoniewska, J. Lach, M. Kacprzak, E. Neczaj, The removal of manganese, iron and ammonium nitrogen on impregnated activated carbon, Desalination 206 (2007) 251–258.
[13] M. Sarioglu, Removal of ammonium from municipal wastewater using natural Turkish (Dogantepe) zeolite, Sep. Purif. Technol. 41 (2005) 1–11.
[14] G. Crini, Recent developments in polysaccharide-based materials used as adsorbents in wastewater treatment, Prog. Polym. Sci. 30 (2005) 38–70.
[15] T. Alexandre, R. Marcos, V. Adriano, Removal of methylene blue dye from an aqueous media using superabsorbent hydrogel supported on modified polysaccharide, J. Colloid Interface Sci. 301 (2006) 55–62.
[16] M.R. Guilherme, A.V. Reis, A.T. Paulino, A.R. Fajardo, E.C. Muniz, E.B. Tambourgi, Superabsorbent hydrogel based on modified polysaccharide for removal of Pb^{2+} and Cu^{2+} from water with excellent performance, J. Appl. Polym. Sci. 105 (2007) 2903–2909.
[17] J. Zhang, Q. Wang, A. Wang, Synthesis and characterization of chitosan-*g*-poly(acrylic acid)/attapulgite superabsorbent composites, Carbohydr. Polym. 68 (2007) 367–374.
[18] I.D. Mall, V.C. Srivastava, G.V.A. Kumar, I.M. Mishra, Characterization and utilization of mesoporous fertilizer plant waste carbon for adsorptive removal of dyes from aqueous solution, Colloids Surf. A: Physicochem. Eng. Aspects 278 (2006) 175–187.
[19] J.W. Lee, S.Y. Kim, Y.M. Lee, K.H. Lee, S.J. Kim, Synthesis and characteristics of interpenetrating polymer network hydrogel composed of chitosan and poly(acrylic acid), J. Appl. Polym. Sci. 73 (1999) 113–120.
[20] Y. Zheng, T. Gao, A. Wang, Preparation, swelling, and slow-release characteristics of superabsorbent composite containing sodium humate, Ind. Eng. Chem. Res. 47 (2008) 1766–1773.
[21] H. Ye, F. Chen, Y. Sheng, G. Sheng, J. Fu, Adsorption of phosphate from aqueous solution onto modified palygorskites, Sep. Purif. Technol. 50 (2006) 283–290.
[22] M. Lebedynets, M. Sprynskyy, I. Sakhnyuk, R. Zbytniewski, R. Golembiewski, B. Buszewski, Adsorption of ammonium ions onto a natural zeolite: transcarpathian clinoptilolite, Adsorpt. Sci. Technol. 22 (2004) 731–741.
[23] H. Zheng, L. Han, H. Ma, Y. Zheng, H. Zhang, D. Liu, S. Liang, Adsorption characteristics of ammonium ion by zeolite 13X, J. Hazard. Mater. 158 (2008) 577–584.
[24] P.H. Nielsen, Adsorption of ammonium to activated sludge, Water Res. 30 (1996) 762–764.
[25] L. Yuan, T. Kusuda, Adsorption of ammonium and nitrate ions by poly(N-isopropylacrylamide) gel and poly(N-isopropylacrylamide-co-chlorophyllin) gel in different states, J. Appl. Polym. Sci. 96 (2005) 2367–2372.

[26] T.C. Chandra, M.M. Mirna, Y. Sudaryanto, S. Ismadji, Adsorption of basic dye onto activated carbon prepared from durian shell: studies of adsorption equilibrium and kinetics, Chem. Eng. J. 127 (2007) 121–129.

[27] E.N. El Qada, S.J. Allen, G.M. Walker, Adsorption of basic dyes from aqueous solution onto activated carbons, Chem. Eng. J. 135 (2008) 174–184.

[28] A.H. Chen, S.C. Liu, C.Y. Chen, C.Y. Chen, Comparative adsorption of Cu(II), Zn(II), and Pb(II) ions in aqueous solution on the crosslinked chitosan with epichloro-hydrin, J. Hazard. Mater. 154 (2008) 184–191.

[29] H. Chen, A. Wang, Adsorption characteristics of Cu(II) from aqueous solution onto poly(acrylamide)/attapulgite composite, J. Hazard. Mater. 165 (2009) 223–231.